

Reversal of ocean acidification enhances net coral reef calcification

Rebecca Albright¹, Lilian Caldeira¹, Jessica Hosfelt², Lester Kwiatkowski¹, Jana K. Maclaren^{1,3}, Benjamin M. Mason⁴, Yana Nebuchina¹, Aaron Ninokawa², Julia Pongratz^{1,5}, Katharine L. Ricke^{1,6}, Tanya Rivlin^{7,8}, Kenneth Schneider^{1,9}, Marine Sesboüé¹, Kathryn Shamberger^{10,11}, Jacob Silverman¹², Kennedy Wolfe¹³, Kai Zhu^{1,14,15} & Ken Caldeira¹

Approximately one-quarter of the anthropogenic carbon dioxide released into the atmosphere each year is absorbed by the global oceans, causing measurable declines in surface ocean pH, carbonate ion concentration ($[\text{CO}_3^{2-}]$), and saturation state of carbonate minerals (Ω). This process, referred to as ocean acidification, represents a major threat to marine ecosystems, in particular marine calcifiers such as oysters, crabs, and corals. Laboratory and field studies^{2,3} have shown that calcification rates of many organisms decrease with declining pH, $[\text{CO}_3^{2-}]$, and Ω . Coral reefs are widely regarded as one of the most vulnerable marine ecosystems to ocean acidification, in part because the very architecture of the ecosystem is reliant on carbonate-secreting organisms⁴. Acidification-induced reductions in calcification are projected to shift coral reefs from a state of net accretion to one of net dissolution this century⁵. While retrospective studies show large-scale declines in coral, and community, calcification over recent decades^{6–12}, determining the contribution of ocean acidification to these changes is difficult, if not impossible, owing to the confounding effects of other environmental factors such as temperature. Here we quantify the net calcification response of a coral reef flat to alkalinity enrichment, and show that, when ocean chemistry is restored closer to pre-industrial conditions, net community calcification increases. In providing results from the first seawater chemistry manipulation experiment of a natural coral reef community, we provide evidence that net community calcification is depressed compared with values expected for pre-industrial conditions, indicating that ocean acidification may already be impairing coral reef growth.

The aragonite saturation state (Ω_{arag}) of tropical surface waters has decreased from about 4.5 in pre-industrial time¹³ to approximately 3.8 by 1995 (ref. 14). In this study, sodium hydroxide (NaOH) was used to increase the total alkalinity of seawater flowing over a reef flat, with the aim of increasing $[\text{CO}_3^{2-}]$ and Ω_{arag} closer to values that would have been attained under pre-industrial levels of atmospheric CO_2 partial pressure (p_{CO_2}). We used a dual tracer regression method to estimate changes in alkalinity uptake (that is, net community calcification) in response to alkalinity addition. This approach uses the change in ratios between an active tracer (alkalinity) and a passive tracer (a non-reactive dye, Rhodamine WT) to assess the fraction of added alkalinity taken up by the reef. Changes in the active tracer (alkalinity) result from mixing, dilution, and biological activity (that is, calcification), whereas changes in the passive tracer (hereafter referred to as the 'dye') are due solely to mixing and dilution. By comparing the alkalinity to dye ratios before (upstream of the study site) and after (downstream) the water mass

interacts with the reef, we were able to isolate the change in alkalinity that is due to an induced increase in net calcification (Extended Data Fig. 1).

Our study was conducted on One Tree Reef (23° 30' S, 152° 06' E), a pseudo-atoll in the southern Great Barrier Reef (Fig. 1a). One Tree Reef encloses three lagoons, two of which are hydrologically distinct (that is, separated by reef walls). At low tide, the water level drops below the outer reef crest, and the lagoons are effectively isolated from the ocean (Fig. 1c). Because First Lagoon sits approximately 30 cm higher than Third Lagoon, gravity-driven, unidirectional flow results from First Lagoon, over the reef flat separating the two lagoons, and into Third Lagoon. Our study site was situated along a section of the reef wall separating First and Third Lagoons. Unidirectional flow across this area of the reef flat persists for approximately 60 min following peak low tide, enabling an experimental setup depicted in Fig. 1d. This section of the reef flat is a well-developed, mixed reef community characterized by ~17% live coral (Extended Data Fig. 2).

Our study was conducted once per day, over 22 days between the dates of 16 September 2014 and 10 October 2014. Dates, times, light data, and predicted heights of low tides are provided in Extended Data Table 1. Before low tide each day, a 15 m³ tank was deployed in First Lagoon, adjacent to the study site. On all 22 days, 4 g Rhodamine WT were mixed with ambient seawater inside the tank. On 15 of those days (hereafter referred to as 'experiment' days), 15 mol (600 g) of NaOH was also introduced into the tank. The resulting solution was pumped onto the reef flat at a constant rate of ~2 l s⁻¹ for 60 min starting at the predicted time of low tide. The resulting plume flowed over the reef flat as described in the Methods. Following the 60 min pumping period, discrete water samples were taken at pre-defined sampling locations along the length of two parallel transects that defined the borders of the study area (along the upstream and downstream edges of the reef flat; Fig. 1d and Extended Data Fig. 3). Samples were analysed for total alkalinity, rhodamine, pH, dissolved inorganic carbon, and nutrients, as described in the Methods (Supplementary Table 1). On 7 days, observations were made when dye, but no alkalinity, was added (hereafter referred to as 'control days'), to test whether the dye addition had unexpected effects, and to characterize background variability in the study area. Mean chemical conditions for control and experimental days are provided in Fig. 2 and Extended Data Fig. 4. On experiment days, the mean concentration of added alkalinity in the central part of the plume (containing 50% of the dye), was $50.2 \pm 2.7 \mu\text{mol kg}^{-1}$, resulting in an average elevation of Ω_{arag} in this part of the plume by 0.6 units. Mean temperatures, salinities, nutrient concentrations,

¹Department of Global Ecology, Carnegie Institution for Science, Stanford, California 94305, USA. ²Bodega Marine Laboratory, University of California, Davis, Bodega Bay, California 94923, USA. ³Stanford Nano Shared Facilities, Stanford University, Stanford, California 94305, USA. ⁴Department of Genetics, Stanford University School of Medicine, Stanford, California 94305, USA. ⁵Max Planck Institute for Meteorology, Bundesstraße 53, 20146 Hamburg, Germany. ⁶Sibley School of Mechanical and Aerospace Engineering, Cornell University, Ithaca, New York 14853, USA. ⁷The Interuniversity Institute for Marine Sciences, The H. Steinitz Marine Biology Laboratory, The Hebrew University of Jerusalem, Eilat, Israel. ⁸The Fredy and Nadine Herrman Institute of Earth Sciences, The Hebrew University of Jerusalem, Edmond J. Safra Campus, Jerusalem, Israel. ⁹Robert H. Smith Faculty of Agriculture, Food and Environment, The Hebrew University of Jerusalem, Rehovot, Israel. ¹⁰Woods Hole Oceanographic Institution, Woods Hole, Massachusetts 02543, USA. ¹¹Texas A&M University, College Station, Texas 77843, USA. ¹²Institute for Oceanographic and Limnological Research, Haifa, Israel. ¹³School of Medical Sciences, The University of Sydney, Sydney, New South Wales 2006, Australia. ¹⁴Department of Biology, Stanford University, Stanford, California 94305, USA. ¹⁵Department of BioSciences, Rice University, Houston, Texas 77005, USA.

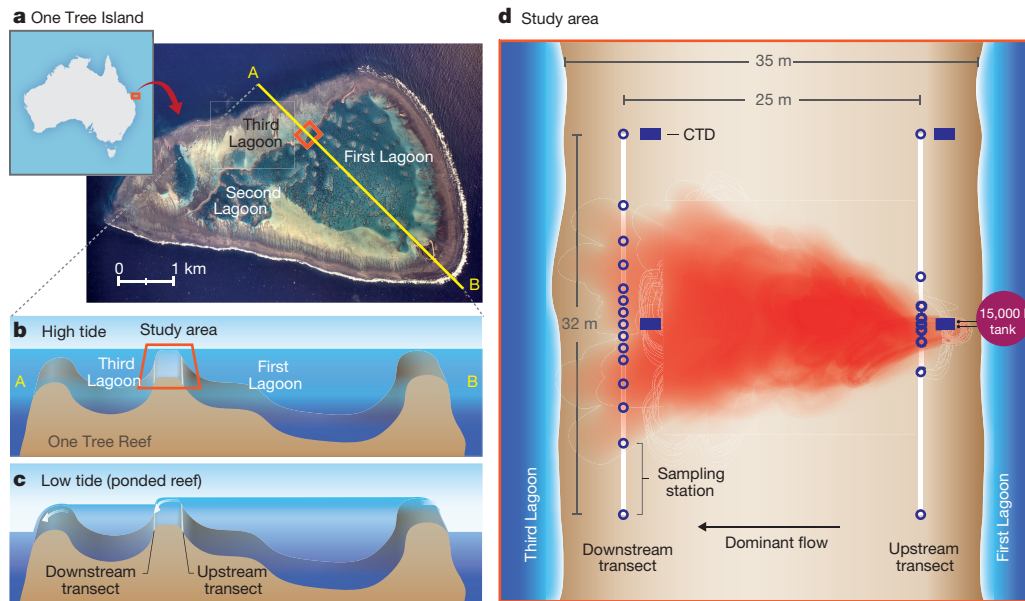


Figure 1 | Study site and experimental design. **a**, Map of Australia and aerial photograph of One Tree Reef with the study area denoted by an orange square. The map, sourced under Creative Commons CC0, is freely available for commercial use. Use of the photograph was permitted under an Educational license from the University of Sydney. **b, c**, Cross-sections

of the reef along the yellow line are shown for high (**b**) and low (**c**) tides, demonstrating the unidirectional flow from the upper lagoon (First Lagoon), over the reef flat study area, and into the lower lagoon (Third Lagoon) during low tide. **d**, Schematic of the study area (to scale) indicating the positioning of the transects and sampling locations (blue circles).

and dissolved oxygen concentrations are provided in Extended Data Table 2.

Plots of the alkalinity and dye concentrations along the upstream and downstream transects illustrate the spatial distribution of the plume within the study area (Fig. 3a–d). On control days, when dye but no alkalinity was added, these parameters were not correlated, and the mean alkalinity–dye slopes did not differ from zero (Fig. 3e). On these days, the difference in alkalinity between the upstream and downstream transects was due to background reef calcification and is represented by the difference in y intercepts. On experiment days, when alkalinity and dye were jointly introduced to the study site, these parameters were well correlated, resulting in positive, significantly non-zero alkalinity–dye slopes both for the upstream and for the downstream transects (Fig. 3f). On these days, background reef calcification is represented by the difference in y intercepts (same as control days), and the fraction of added alkalinity taken up by the reef flat, f_{uptake} , was calculated as the difference between the upstream and downstream alkalinity–dye slopes:

$$f_{\text{uptake}} = 1 - (r_{\text{down}}/r_{\text{up}}) \quad (1)$$

where r_{up} and r_{down} are the ratios (slopes) of alkalinity to dye for the upstream and downstream transects, respectively, in $\mu\text{mol kg}^{-1} \text{ppb}^{-1}$ or mmol g^{-1} . At a fixed rate of alkalinity and dye addition, r_{up} indicates the amount of added alkalinity entering our study site, while r_{down} indicates the amount of added alkalinity leaving our study site. The difference in these two values indicates the amount of added alkalinity taken up by the reef community and was used to calculate the percentage increase in net calcification according to equations (2)–(4).

Data from all days were analysed using a multivariate regression approach to calculate alkalinity–dye ratios (slopes) and mean background alkalinities (y intercepts) of the upstream and downstream transects, while simultaneously accounting for natural spatial and temporal variability (see Supplementary Information and Extended Data Figs 5–7). Mean alkalinity–dye slopes are presented in Fig. 4a. Results of a mixed-effects model indicate that upstream and downstream slopes are significantly different on experiment days but not control days, rejecting the null hypothesis that net community calcification did not respond to alkalization (see Supplementary Information).

The fractional uptake of added alkalinity was calculated according to equation (1) and averaged for all control and experimental days. Using this method, we estimate that an average of $17.3\% \pm 2.3\%$ (1 s.e.m.) of the experimentally added alkalinity was taken up by the reef community.

The percentage increase in net calcification, ΔG , resulting from alkalinity addition was calculated as:

$$\Delta G = G_{\text{increase}}/G_{\text{background}} \quad (2)$$

where G_{increase} is the additional calcification resulting from alkalinity addition in mmol s^{-1} , and $G_{\text{background}}$ is the background calcification in mmol s^{-1} (that is, the calcification rate without added alkalinity). G_{increase} and $G_{\text{background}}$ were calculated as

$$G_{\text{increase}} = P_{\text{dye}}(r_{\text{up}} - r_{\text{down}}) \quad (3)$$

$$G_{\text{background}} = F(\text{Alk}_{\text{up}} - \text{Alk}_{\text{down}}) \quad (4)$$

where P_{dye} is the pumping rate of the dye in g s^{-1} , F is the volumetric flow rate in $\text{m}^3 \text{s}^{-1}$, and Alk_{up} and Alk_{down} are the mean background alkalinities (that is, the y intercepts) of the upstream and downstream transects, respectively, in mmol m^{-3} (see Supplementary Information). Using these equations, we estimate net community calcification increased by an average of $6.9\% \pm 0.9\%$ (Fig. 4b). A one-tailed, unpaired t -test indicates that the change in calcification on experiment days was significantly greater than control days ($t_{20} = 1.981$, $P < 0.05$). On the basis of laboratory and mesocosm studies¹⁵, the mean response of coral calcification to a unit change in Ω_{arag} is approximately 15%. Throughout the entire study area (inside and outside the plume), Ω_{arag} was elevated by an average of 0.4 units, indicating a theoretical increase in coral calcification of 6%, which agrees closely with the observed increase of 6.9%. Caution must be applied, however, when comparing calcification relationships derived from coral studies¹⁵ to mixed-reef communities such as that of our study site.

The hypothesis that Ω_{arag} exerts strong control over coral reef calcification is supported by laboratory experiments and models^{16,17} (but see ref. 18); however, isolating this control in a natural setting is complicated by the multiple drivers of calcification, which are often highly

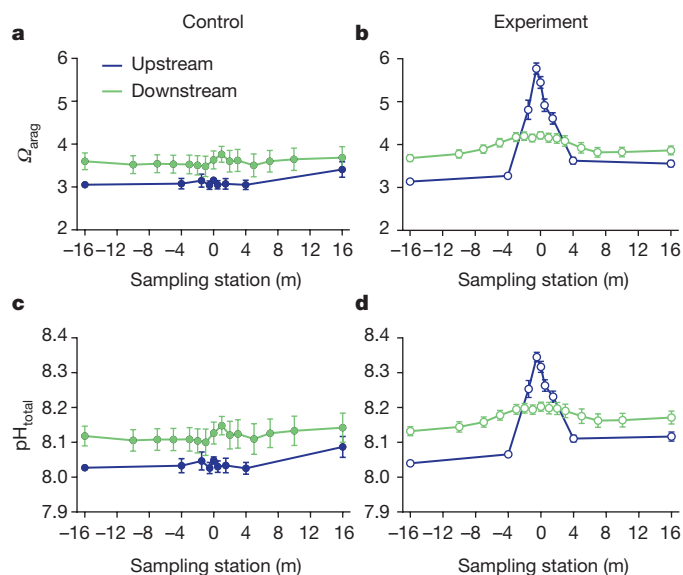


Figure 2 | Chemical conditions for control ($N = 7$) and experiment ($N = 15$) days (mean \pm 1 s.e.m.). a, b, Aragonite saturation states (Ω_{arag}); c, d, pH. Error bars are indicative of day-to-day and hour-to-hour variability (not measurement error); estimated measurement errors are smaller than line thickness and are provided in the Methods. Experimental day standard errors are smaller than control day standard errors primarily because of the larger N .

correlated (for example, production, Ω_{arag} , light, temperature)^{6,12,19–24}. Previous attempts to manipulate seawater chemistry in the natural environment were unable to demonstrate a causal relationship between seawater chemistry and reef calcification²⁵. Further, retrospective studies documenting declines in coral reef calcification over the past several decades were unable to isolate the influences of various causal factors (for example, ocean warming, acidification, water quality, fishing pressure) owing to the confounding influence of co-varying parameters and a lack of reliable long-term carbonate chemistry observations^{7,26}. Our experimental approach demonstrates the influence of alkalinity (and Ω_{arag}) on net community calcification in a natural setting by uncoupling Ω_{arag} from otherwise co-varying confounding environmental factors (where ‘uncouple’ is used in the technical sense of ‘lack of correlation’). We demonstrate that restoring $[\text{CO}_3^{2-}]$ and Ω_{arag} closer to pre-industrial values enhances net community calcification, providing evidence that ocean acidification may have contributed to the documented declines in coral reef calcification^{6–12} in the industrial era.

Notably, ocean acidification is one of many stressors acting on coral reef calcification. Simultaneously to decreasing Ω_{arag} , sea surface temperatures have warmed by an estimated 0.4–0.8 °C (varying by region) since the early 1800s (ref. 27) which is posited to have increased calcification rates until a recent ‘tipping point’²⁸. Identifying the relative contributions of various environmental factors, and how they interact, to the documented declines in coral reef calcification is complex yet essential to understanding how calcification will probably change in the coming decades. Further work, using methods developed here, could examine how coral reef response is affected by a variety of stressors (in isolation and combination) and duration of exposure, and help to assess geographic variability in sensitivity to ongoing ocean acidification.

The Ω_{arag} of the tropical oceans is expected to continue declining from 3.8 to approximately 3.0 by the middle of the century and 2.3 by the end of the century¹⁴. Deliberate alkalization has been proposed as a geoengineering technique to offset ocean acidification impacts on coral reefs and other shallow marine ecosystems²⁹. Our results indicate that this approach could, in principle, help protect coral reefs from ocean acidification; however, the technical challenges associated with implementation would probably make it infeasible at anything but

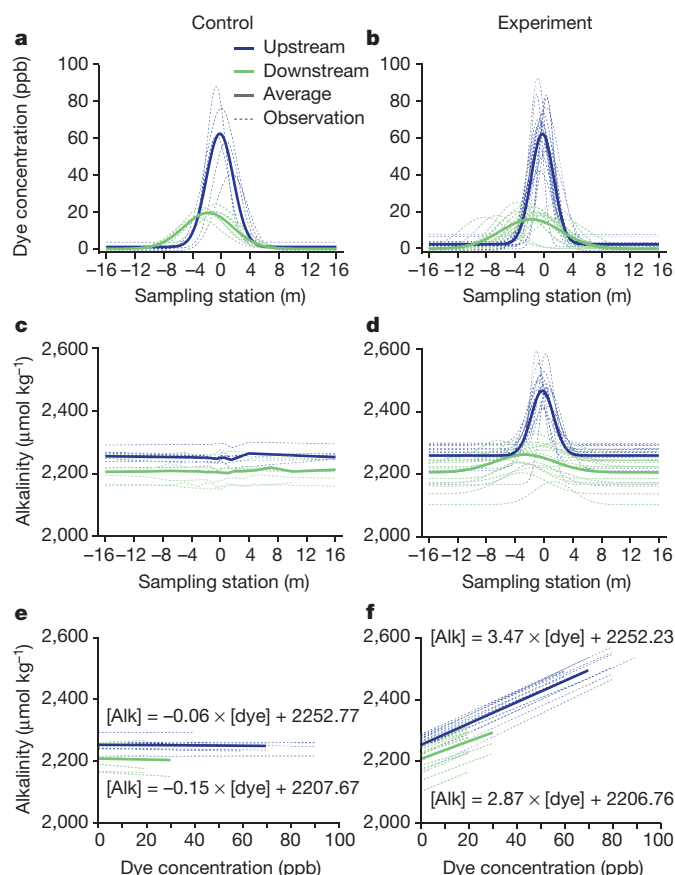


Figure 3 | Relationships between alkalinity and dye for control ($N = 7$) and experiment ($N = 15$) days. a, b, Dye concentrations; c, d, alkalinities; e, f, alkalinity–dye slopes. e, On control days, when dye, but no NaOH, was added to the study site, these parameters are not correlated, and the resulting alkalinity–dye slopes are not significantly different from zero. f, On experimental days, dye and NaOH were jointly added to the study site, and the correlation between these parameters results in a positive, significantly non-zero slope. Mean alkalinity–dye slopes for control and experiment days are shown in Fig. 4a.

highly localized scales (for example, protected bays, lagoons). Large-scale and long-term protection of marine ecosystems from the threat of ocean acidification depends on deep and rapid reductions in anthropogenic emissions of carbon dioxide³⁰.

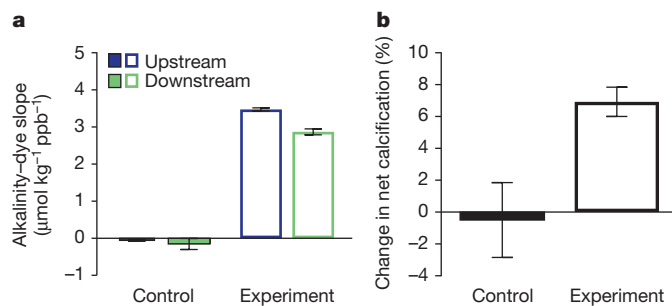


Figure 4 | Alkalinity–dye slopes and percentage change in net calcification for control ($N = 7$) and experiment ($N = 15$) days (mean \pm 1 s.e.m.). a, b, The difference between upstream and downstream slopes (a) was used to calculate the uptake of added alkalinity (equation (1)) and the percentage change in net calcification (b) (equations (2)–(4)). The reef community took up an average of $17.3\% \pm 2.3\%$ of the added alkalinity, implying a $6.9 \pm 0.9\%$ increase in net calcification. The percentage change in calcification on experiment days was significantly greater than control days (one-tailed, unpaired t -test, $t_{20} = 1.981$, $P < 0.05$). Results by day are presented in Extended Data Fig. 7.

Online Content Methods, along with any additional Extended Data display items and Source Data, are available in the online version of the paper; references unique to these sections appear only in the online paper.

Received 29 September 2015; accepted 20 January 2016.

Published online 24 February 2016.

- Le Quéré, C. *et al.* Global carbon budget 2014. *Earth System Science Data* **7**, 47–85 (2015).
- Fabry, V. J., Seibel, B. A., Feely, R. A. & Orr, J. C. Impacts of ocean acidification on marine fauna and ecosystem processes. *ICES J. Mar. Sci.* **65**, 414–432 (2008).
- Doney, S. C., Fabry, V. J., Feely, R. A. & Kleypas, J. A. Ocean acidification: the other CO₂ problem. *Annu. Rev. Mar. Sci.* **1**, 169–192 (2009).
- Andersson, A. J. & Gledhill, D. Ocean acidification and coral reefs: effects on breakdown, dissolution, and net ecosystem calcification. *Annu. Rev. Mar. Sci.* **5**, 321–348 (2013).
- Silverman, J., Lazar, B., Cao, L., Caldeira, K. & Erez, J. Coral reefs may start dissolving when atmospheric CO₂ doubles. *Geophys. Res. Lett.* **36**, (2009).
- Silverman, J. *et al.* Community calcification in Lizard Island, Great Barrier Reef: a 33 year perspective. *Geochim. Cosmochim. Acta* **144**, 72–81 (2014).
- De'ath, G., Lough, J. M. & Fabricius, K. E. Declining coral calcification on the Great Barrier Reef. *Science* **323**, 116–119 (2009).
- Cooper, T. F., De'Ath, G., Fabricius, K. E. & Lough, J. M. Declining coral calcification in massive *Porites* in two nearshore regions of the northern Great Barrier Reef. *Glob. Change Biol.* **14**, 529–538 (2008).
- Manzello, D. P. Coral growth with thermal stress and ocean acidification: lessons from the eastern tropical Pacific. *Coral Reefs* **29**, 749–758 (2010).
- Cantin, N. E., Cohen, A. L., Karnauskas, K. B., Tarrant, A. M. & McCorkle, D. C. Ocean warming slows coral growth in the central Red Sea. *Science* **329**, 322–325 (2010).
- Tanzil, J. T. *et al.* Regional decline in growth rates of massive *Porites* corals in Southeast Asia. *Glob. Change Biol.* **19**, 3011–3023 (2013).
- Silverman, J. *et al.* Carbon turnover rates in the One Tree Island reef: a 40-year perspective. *J. Geophys. Res.* **117**, G03023 (2012).
- Cao, L. & Caldeira, K. Atmospheric CO₂ stabilization and ocean acidification. *Geophys. Res. Lett.* **35**, (2008).
- Feely, R. A., Doney, S. C. & Cooley, S. R. Ocean acidification: present conditions and future changes in a high-CO₂ world. *Oceanography* **22**, 36–47 (2009).
- Chan, N. C. & Connolly, S. R. Sensitivity of coral calcification to ocean acidification: a meta-analysis. *Glob. Change Biol.* **19**, 282–290 (2013).
- Langdon, C. & Atkinson, M. Effect of elevated pCO₂ on photosynthesis and calcification of corals and interactions with seasonal change in temperature/irradiance and nutrient enrichment. *J. Geophys. Res.* **110**, C09S07 (2005).
- Kroeker, K. J., Kordas, R. L., Crim, R. N. & Singh, G. G. Meta-analysis reveals negative yet variable effects of ocean acidification on marine organisms. *Ecol. Lett.* **13**, 1419–1434 (2010).
- Cyronak, T., Schulz, K. G. & Jokiel, P. L. The Omega myth: what really drives lower calcification rates in an acidifying ocean. *ICES J. Mar. Sci.* <http://dx.doi.org/10.1093/icesjms/fsv075> (2015).
- Shaw, E. C., Phinn, S. R., Tilbrook, B. & Steven, A. Natural in situ relationships suggest coral reef calcium carbonate production will decline with ocean acidification. *Limnol. Oceanogr.* **60**, 777–788 (2015).
- Albright, R., Benthuysen, J., Cantin, N., Caldeira, K. & Anthony, K. Coral reef metabolism and carbon chemistry dynamics of a coral reef flat. *Geophys. Res. Lett.* **42**, 3980–3988 (2015).
- Kowek, D. *et al.* Environmental and ecological controls of coral community metabolism on Palmyra Atoll. *Coral Reefs* **34**, 339–351 (2014).
- Shaw, E. C., McNeil, B. I. & Tilbrook, B. Impacts of ocean acidification in naturally variable coral reef flat ecosystems. *J. Geophys. Res.* **117**, C03038 (2012).
- Albright, R., Langdon, C. & Anthony, K. R. N. Dynamics of seawater carbonate chemistry, production, and calcification of a coral reef flat, central Great Barrier Reef. *Biogeosciences* **10**, 6747–6758 (2013).
- Falter, J. L., Lowe, R. J., Zhang, Z. & McCulloch, M. Physical and biological controls on the carbonate chemistry of coral reef waters: effects of metabolism, wave forcing, sea level, and geomorphology. *PLoS ONE* **8**, e53303 (2013).
- Kline, D. I. *et al.* A short-term *in situ* CO₂ enrichment experiment on Heron Island (GBR). *Sci. Rep.* **2**, 413 (2012).
- Helmle, K. P., Dodge, R. E., Swart, P. K., Gledhill, D. K. & Eakin, C. M. Growth rates of Florida corals from 1937 to 1996 and their response to climate change. *Nature Commun.* **2**, 215 (2011).
- Tierney, J. E. *et al.* Tropical sea surface temperatures for the past four centuries reconstructed from coral archives. *Paleoceanography* **30**, 226–252 (2015).
- Lough, J. M. & Cooper, T. F. New insights from coral growth band studies in an era of rapid environmental change. *Earth Sci. Rev.* **108**, 170–184 (2011).
- National Research Council. *Climate Intervention: Carbon Dioxide Removal and Reliable Sequestration* (National Academies Press, 2015).
- Ricke, K. L., Orr, J. C., Schneider, K. & Caldeira, K. Risks to coral reefs from ocean carbonate chemistry changes in recent earth system model projections. *Environ. Res. Lett.* **8**, 034003 (2013).

Supplementary Information is available in the online version of the paper.

Acknowledgements We thank R. Dunbar for the use of his laboratory and D. Mucciarone for laboratory training and assistance; the Australian Institute of Marine Science for scientific and technical support; Y. Estrada for graphics assistance; and the following people for their support in the field and/or laboratory: M. Byrne, A. Chai, R. Graham, T. Hill, D. Kline, B. Kravitz, J. Reiffel, D. Ross, E. Shaw, and the staff of the One Tree Island Research Station. Expedition and staff support was provided by the Carnegie Institution for Science. Some additional support for staff, but not expedition expenses, was provided by the Fund for Innovative Climate and Energy Research. This work was permitted by the Great Barrier Reef Marine Park Authority under permit G14/36863.1.

Author Contributions R.A., J.K.M., K.Sc., J.S., and K.C. conceived and designed the project. J.K.M., K.Sc., J.S., J.P., K.L.R., and K.Sh. conducted pilot studies and collected preliminary data. R.A., L.K., L.C., B.M.M., Y.N., T.R., M.S., K.W., A.N., J.H., and K.C. performed the experiments. R.A. and K.C. performed the computational analyses. K.Z. assisted with statistical analyses. R.A. wrote the manuscript with input from K.C. All co-authors reviewed and approved the final manuscript.

Author Information Reprints and permissions information is available at www.nature.com/reprints. The authors declare no competing financial interests. Readers are welcome to comment on the online version of the paper. Correspondence and requests for materials should be addressed to R.A. (ralbright@carnegiescience.edu).

METHODS

No statistical methods were used to predetermine sample size. The experiments were not randomized. The investigators were not blinded to allocation during experiments and outcome assessment.

Concept. The dual tracer regression method developed here is an extension of ref. 31 and may have applications in other areas of research, such as nutrient or pollution assessments, uptake of industrial or agricultural waste, etc. The primary experimental criteria are that the active and passive tracers are added in a fixed ratio and at a fixed rate. The methods described here apply to situations where there is a dominant flow direction, dispersion or dilution, and a need to measure the effect of a reagent on community flux.

Experimental setup. Before low tide each day, a 15 m³ floating 'header' tank was partly submerged in First Lagoon, adjacent to the reef flat study site. The tank was gravity-fed with ambient seawater from the lagoon, and when necessary, a submersible pump was used to completely fill the tank. Two marine grade bilge pumps (3,000 gallons per hour, Five Oceans) were secured inside the tank for mixing during chemical addition and to deliver the solution to the study site. On 22 days, 4g Rhodamine WT (20 g of a 20% solution, Turner Designs 10–108), dissolved in 0.5 l reverse osmosis (RO) water, was manually added to the tank over the course of ~30 min and mixed. On 15 of those days, 600 g (~15 mol) of NaOH, dissolved in 1.5 l RO water, was also introduced into the tank. The solution inside the tank was subsequently mixed for an additional 30–45 min to ensure homogeneity. When a strong source of alkalinity is added to seawater, brucite forms as a solid precipitate. However, for pH levels below ~9, brucite dissolves. On the basis of visual inspection and associated laboratory experiments, we estimated brucite dissolution to occur on the timescale of ~100 s. Therefore, a mixing time of 30–45 min was sufficient to ensure complete dissolution of brucite; during this time, a handheld pH probe (Oakton) was used to manually check that the pH of the tank solution did not exceed 9.0. The tank was covered to avoid equilibration with the atmosphere, but given that the tank was emptied over a period of 60 min, it is possible that air–sea fluxes were not completely avoided. While acid/base manipulations of seawater carbonate chemistry are not directly equivalent to the addition/removal of dissolved inorganic carbon (C_T), the differences in carbon speciation between acid/base manipulations and CO₂ gas manipulations are minor if seawater is not allowed to equilibrate with the atmosphere (that is, in closed or continuous-flow systems). Further, it is infeasible to remove CO₂ from large volumes of seawater (>10,000 l) under field conditions. Therefore, acid/base manipulations are considered justified techniques to alter seawater carbonate chemistry in circumstances where large volumes of seawater are being manipulated, such as mimicking natural flow on coral reefs, particularly if the system is not allowed to equilibrate with the atmosphere³².

The seawater solution from the tank (control days: seawater + dye; experiment days: seawater + NaOH + dye) was pumped onto the reef flat for a period of 60 min starting at the predicted time of low tide (Extended Data Table 1) at a constant rate (~21 s⁻¹). The solution was introduced to the study site via the two bilge pumps that were submerged in the tank, connected to two lengths of (1.5-inch inner diameter) vinyl tubing that were secured to a cinder block located ~2 m upstream from the centre of the study site. Throughout the addition, the ratio of alkalinity to dye being added to the study site was assumed to be constant, and flow within the study site was considered to be in steady-state. On 30 September 2014 (a control day), dye was added using a peristaltic pump instead of the above configuration; this was because low tide occurred at 5:32, and assembly of the tank configuration was not possible in low-light conditions.

Following a pumping period of 60 min, discrete water samples were taken at defined sampling locations along the length of two parallel transects that defined the borders of the study area: one along the upstream edge (adjacent to First Lagoon) and the other along the downstream edge (adjacent to Third Lagoon, see Extended Data Fig. 3). The total width of the reef flat in this area is approximately 35 m, and the upstream and downstream transects were separated by ~25 m. The length of each transect was 32 m. Thus, the study area consisted of an approximate 25 m × 32 m rectangle (800 m²). The upstream transect consisted of 9 sampling stations spanning the width of 32 m, and the downstream transect consisted of 15 sampling stations spanning the width of 32 m. Sample locations were strategically assigned with a higher density near the centre of the study area to accurately characterize the shape of the resulting alkalinity and dye plume/curve. Spacing of the station locations is depicted in Extended Data Fig. 3.

Following the 60 min pumping period, discrete samples were collected at each of the 24 sample locations by pumping reef water into 500 ml borosilicate glass bottles (Corning, 1500–500 Pyrex glass reagent bottle) using battery-operated liquid transfer pumps (Sierra Tools, model JB5684). To minimize chemical variation due to minor changes in sampling depth and/or location, precise sample locations were marked with plastic discs, nailed to the reef substrate. Samples were collected along the upstream and downstream transects simultaneously by five individuals, with

each person sampling four or five locations. All samples were typically collected in less than 3 minutes, and it was assumed that the study site was in steady state during this time (that is, all fluxes and flows did not change during the 3-minute sampling interval). Samples were immediately returned to the One Tree Island Research Station, where they were subsampled and analysed for pH, total alkalinity (A_T), dissolved inorganic carbon (C_T), and rhodamine (see 'Chemical Analyses' section). For three upstream stations (–U16, U0, U16) and three downstream stations (–D16, D0, D16), nitrate and ammonia concentrations were also determined. See Extended Data Fig. 3 for station locations.

CTD (conductivity–temperature–depth) devices (YSI models 6600, 6920) were deployed at four sampling locations, two upstream (–U16, U0) and two downstream (–D16, D0) for continuous measurements of seawater temperature, salinity, depth, and dissolved oxygen concentration. These instruments logged continuously at 2-minute intervals over the 22 study days. Discrete water samples (Corning, 1500–250 Pyrex glass reagent bottle) were collected each day at each of the four CTD locations, and the dissolved oxygen concentration was measured using an automated potentiometric Winkler titration technique³³. These values were used to verify CTD measurements.

Alkalinity–dye slopes, r , and mean background alkalinities, \hat{a} , for each day were calculated using paired alkalinity and dye measurements that were collected across all sampling stations, transects, and days (see Supplementary Information). Over a 4-week period, we conducted our experimental protocol 23 times: 8 control days and 15 experimental days. One control day was omitted from subsequent analyses owing to intense rain that heavily influenced alkalinity measurements, resulting in 7 control days and 22 total days. This resulted in a total of 526 paired alkalinity and dye measurements that were used in the fitting procedure described in the Supplementary Information. Two previous expeditions to One Tree Island (September/October 2012 and March 2013) characterized site variability and allowed testing of the methods presented here. Preliminary data generated in these expeditions indicated that demonstrating statistical significance was dependent on maximizing signal (uptake of experimentally added alkalinity) to noise (natural/background uptake of alkalinity).

On experiment days, the difference between the upstream and downstream alkalinity–dye slopes indicates the fraction of experimentally added alkalinity that was taken up by the reef (equation (1) of the main text). We analysed the difference between slopes using a mixed-effects model in R (see Supplementary Information). Comparison of confidence intervals indicates that upstream and downstream slopes are significantly different on experiment days but not on control days. Shapiro–Wilk W -tests were used to verify the underlying assumptions of normality ($P > 0.05$). The purpose of control days was to demonstrate that significant changes in alkalinity–dye slopes do not occur when NaOH is not added, and to characterize natural spatial and temporal variability in the study site. Further, with this study methodology, effectively, within experimental days, the part of the study site that is not affected by the alkalinity-rich plume serves as additional control for the part of the study site that is affected by the plume.

While reef processes other than calcification can alter seawater alkalinity (for example, changes in nutrients, salinity), a previous study showed that changes in salinity and nutrients had a negligible effect on changes in alkalinity in coral reefs³⁴. Salinity and nutrient data from our study are provided in Extended Data Table 2. **Code availability.** The Mathematica routine used to calculate alkalinity-to-dye ratios (slopes) and dye-free mean alkalinity estimates (y intercepts) for each day is provided in the Supplementary Information.

Chemical analyses. Discrete samples were immediately returned to the laboratory on One Tree Island where they were analysed for pH_{total}, total alkalinity (A_T), and rhodamine, and subsampled for the later determination of total dissolved inorganic carbon (C_T), and nutrients (NH₄⁺, NO₂, and NO₃). All measurements and calculations were consistent with 'best practices' recommendations³⁵. For 99.6% of station–day combinations (24 stations × 22 days = 528 bottles), we successfully measured pH_{total}, A_T, rhodamine, and C_T, resulting in 526 paired measurements.

Aragonite saturation state (Ω_{arag}), carbonate ion concentration ($[\text{CO}_3^{2-}]$), and $p\text{CO}_2$ were calculated as a function of A_T, pH_{total}, and *in situ* salinity and temperature using the program CO2SYS³⁶; dissociation constants for carbonate and boric acid were determined as in ref. 37 and as refitted in ref. 38, and the dissociation constant for boric acid was determined as in ref. 39.

Parameters that were measured at a subset of sampling stations (that is, temperature, salinity, and dissolved oxygen measured at –U16, U0, –D16, D0; nutrients measured at –U16, U0, U16, –D16, D0, D16) are presented in Extended Data Table 2. Parameters that were measured (or calculated) across all sampling stations are presented in Fig. 2 (Ω_{arag} and pH) and Extended Data Fig. 4 (CO₃²⁻, $p\text{CO}_2$, and C_T). All chemistry data are included in Supplementary Table 1.

Total alkalinity, A_T. Samples for A_T were pre-filtered using GF/F filters (Whatman) and analysed in triplicate using a Metrohm 855 Robotic Titrosampler (Metrohm

USA) using certified 0.1 N HCl (Fisher Chemical) diluted to a nominal concentration of 0.0125 N. Acid was calibrated by analysing certified reference material (CRM, batch 138) from A. Dickson's laboratory before each titration session (twice daily). A_T by volume ($\mu\text{mol l}^{-1}$) was converted to A_T by mass ($\mu\text{mol kg}^{-1}$) by applying a density correction using *in situ* salinities and temperatures. For each set of triplicate analyses, data points that were $>10 \mu\text{mol kg}^{-1}$ away from the median were removed from the analysis; these outliers resulted from drop scale variability in sample delivery. The resulting mean and standard error were calculated for each sample location on each day. Instrumental precision from 55 analyses of CRM (batch 138) over the course of the study was $<2 \mu\text{mol kg}^{-1}$ (1 s.d.). Alkalinities were normalized to the mean salinity of 35.75; salinity-normalized alkalinities were used for subsequent analyses.

pH. Seawater pH_{total} was determined using an Ocean Optics spectrophotometer with 10 cm path length optical cells and *m*-cresol purple dye (Sigma Aldrich), following the methods of ref. 41. Water samples were kept in a temperature-controlled water bath (Thermo Scientific, Precision Microprocessor Controlled 280 Series) at 25 °C before analysis to minimize temperature-induced errors in absorbance measurements. The temperature of each sample was recorded immediately after analysis using a digital thermometer accurate to ± 0.05 °C (VWR, Traceable Platinum Ultra-Accurate Digital Thermometer). CO2SYS³⁶ was used to calculate *in situ* pH values using *in situ* salinity and temperature measurements. Average precision from triplicate measurements for this system was less than 0.010 units (1 s.d.). CRM analyses (TRIS buffer, batch 22, A. Dickson) revealed that the system was accurate to within 0.005 pH units.

Rhodamine WT. Rhodamine WT concentration was measured fluorometrically using a Turner 10AU fluorometer and 25 ml cuvettes. A series of eight standards was made by mass-diluting a 400 ppb (Parts per 10⁹) Rhodamine WT standard (Turner Designs) to 0, 0.5, 1, 2, 4, 16, 32, and 64 ppb. The standard curve was measured at the beginning, middle, and end of each measuring day to check for drift. Water samples were kept in a temperature-controlled water bath (Thermo Scientific, Precision Microprocessor Controlled 280 Series) at 25 °C before analysis to minimize temperature-induced errors in fluorescence. The temperature of each sample was recorded immediately after analysis using a digital thermometer accurate to ± 0.05 °C (VWR, Traceable Platinum Ultra-Accurate Digital Thermometer). Rhodamine concentrations were temperature-corrected using the formula $F_r = F_s \exp(k(T_s - T_r))$, where F_r and F_s are the fluorescence at the reference and sample temperatures, T_r and T_s , and $k = 0.026/\text{K}$, equating to a 2.6% correction per kelvin (ref. 40). Temperature corrections were applied before normalizing values to the standard curve. Dye concentrations were then normalized to the mean salinity of 35.75; salinity-normalized concentrations were used for subsequent analyses. Instrumental precision from triplicate measurements for this system was less than 0.1 ppb.

Dissolved inorganic carbon (C_T). C_T samples were subsampled into 30 ml glass serum bottles (Wheaton, 223743), poisoned with 15 μl saturated HgCl_2 (0.05% by volume to inhibit biological activity⁴¹), sealed with rubber stoppers, crimped closed with aluminium caps, and transported to Stanford University for analysis. Samples were analysed approximately 3 months after sampling. C_T was extracted from samples by acidifying them with phosphoric acid (H_3PO_4 , 5%) using a custom-built, automated acidification and delivery system (D. Mucciarone) using high-grade nitrogen as a carrier gas connected to an infrared gas analyser (Licor 7000). All samples were analysed in duplicate. The instrument was calibrated daily using CRM (Batches 141, 138), provided by A. Dickson. Immediate duplicate analyses of samples usually yielded instrumental precision of 1–2 $\mu\text{mol kg}^{-1}$.

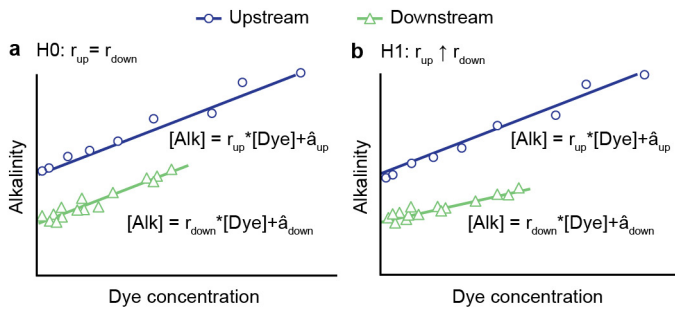
Nutrients. Nutrient samples were subsampled into 15 ml conical centrifuge tubes (Falcon). Ammonia samples were immediately frozen, and total ammonium concentrations ($\text{NH}_3\text{-tot} = \text{NH}_3 + \text{NH}_4^{1+}$) were later determined using a modified fluorometric method⁴². Nitrate samples were preserved with 0.1 ml 1 N HCl, closed, shaken, and left in the dark at room temperature (~ 22 °C) until transport to Eilat, Israel. Nitrite (NO_2^{1-}) was measured using a colorimetric method⁴³,

with a Flow Injection Autoanalyzer (Lachat Instruments model QuickChem 8500). Nitrate (NO_3^{1-}) was measured by reducing it to nitrite using a copperized cadmium column. Precision of ammonia, nitrite, and nitrate measurements was $\sim 0.05 \mu\text{mol l}^{-1}$. Nitrite and nitrate in this study are reported as total oxidized nitrogen ($\text{TON} = \text{NO}_2^{1-} + \text{NO}_3^{1-}$). Results are provided in Extended Data Table 2.

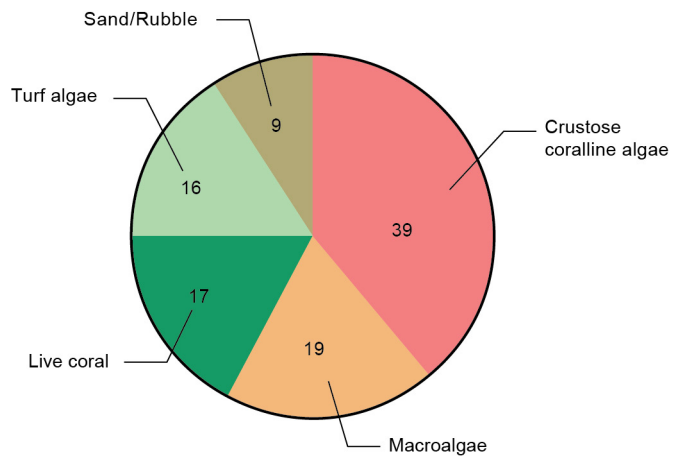
Salinity. Following the first 5 days of observations, it became evident that conductivity measurements from three of the four CTDs proved unreliable; we believed this to be from the formation of oxygen bubbles on the sensors (resulting from high productivity on the reef flat). Therefore, starting on day six, discrete water samples were taken each day at each of the four CTD locations. Samples were stored in an air-conditioned, shaded room until transport to the Australian Institute of Marine Science for analysis on a Guildline Portasal Salinometer (model 8410A), with a precision of ± 0.0001 units. Accuracy was verified using CRM (OSIL, IAPSO Standard Seawater, batch P155). For days without discrete salinity measurements ($N = 5$), salinity values were calculated for the upstream transect by developing a linear relationship between the salinometer values and the reliable CTD. Salinities for the downstream transect were calculated from upstream values by applying an offset of 0.08 parts per thousand; this offset represents the mean increase in salinity between the upstream and downstream transects as a result of evaporation (Extended Data Table 2).

Benthic community structure. Benthic surveys were conducted to characterize the underlying community structure of the study area. Five 25 m transects were laid on the reef flat perpendicular to the reef front, spaced approximately 8 m apart. Photographs were taken of 0.25 m² quadrats at 5 m intervals. Photographs were analysed with Coral Point Count software with Excel extensions (CPCe) using 25 random points per quadrat. The benthos was assigned to one of six categories: (1) live coral; (2) macroalgae; (3) turf algae; (4) *Halimeda*; (5) crustose coralline algae (CCA); and (6) sand/rubble. Where morphological forms of CaCO_3 (for example, rubble, CaCO_3 rock) were covered with biologically active groups (for example, turf, CCA), the biologically active group was scored. Results are provided in Extended Data Fig. 2.

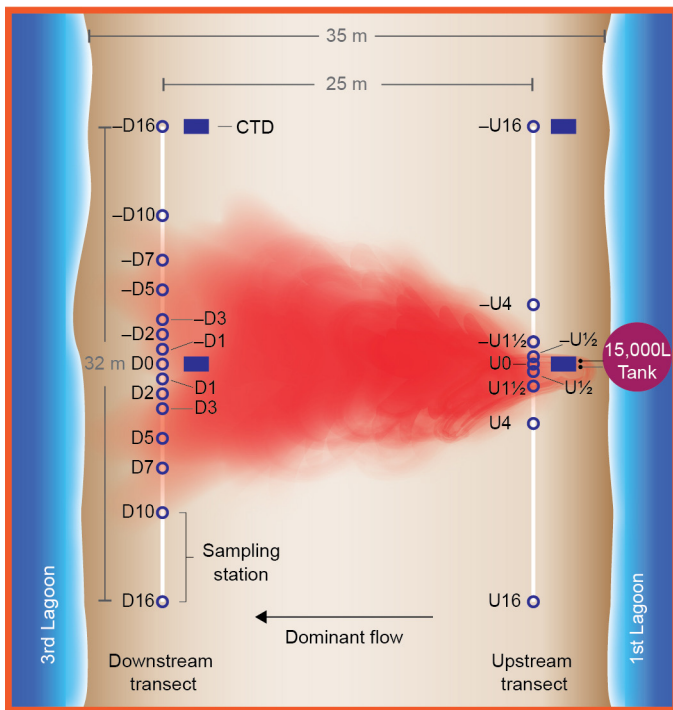
- Friedlander, S. K., Turner, J. R. & Hering, S. V. A new method for estimating dry deposition velocities for atmospheric aerosols. *J. Aerosol Sci.* **17**, 240–244 (1986).
- Andersson, A. J. & Mackenzie, F. T. Revisiting four scientific debates in ocean acidification research. *Biogeosciences* **9**, 893–905 (2012).
- Anderson, L. G., Haraldsson, C. & Lindegren, R. Gran linearization of potentiometric Winkler titrations. *Mar. Chem.* **37**, 179–190 (1992).
- Kinsey, D. Alkalinity changes and coral reef calcification. *Limnol. Oceanogr.* **23**, 989–991 (1978).
- Riebesell, U., Fabry, V. J., Hansson, L. & Gattuso, J. P. *Guide to Best Practices for Ocean Acidification Research and Data Reporting* (Publications Office of the European Union, 2010).
- Lewis, E. & Wallace, D. W. R. Program developed for CO₂ system calculations (US Department of Energy Oak Ridge National Laboratory, 1998).
- Mehrbach, C., Culberson, C. H., Hawley, J. E. & Pytkowicz, R. M. Measurement of the apparent dissociation constants of carbonic acid in seawater at atmospheric pressure. *Limnol. Oceanogr.* **18**, 897–907 (1973).
- Dickson, A. G. & Millero, F. J. A comparison of the equilibrium constants for the dissociation of carbonic acid in seawater media. *Deep-Sea Res.* **34**, 1733–1743 (1987).
- Dickson, A. G. Thermodynamics of the dissociation of boric acid in synthetic seawater from 273.15 to 318.15 K. *Deep-Sea Res.* **37**, 755–766 (1990).
- Wilson, J. F. in *Techniques for Water Resources Investigations of the U.S. Geological Survey*, Book 3, Ch. A12 (U.S. Government Printing Office, 1968).
- Dickson, A. G., Sabine, C. L. & Christian, J. R. *Guide to Best Practices for Ocean CO₂ Measurements* (North Pacific Marine Science Organization, 2007).
- Holmes, R. M., Aminot, A., Kerouel, R., Hooker, B. A. & Peterson, B. J. A simple and precise method for measuring ammonium in marine and freshwater ecosystems. *Can. J. Fish. Aquat. Sci.* **56**, 1801–1808 (1999).
- Grasshoff, K., Kremling, K. & Ehrhardt, M. (eds) *Methods of Seawater Analysis* (Wiley-VCH, 1999).



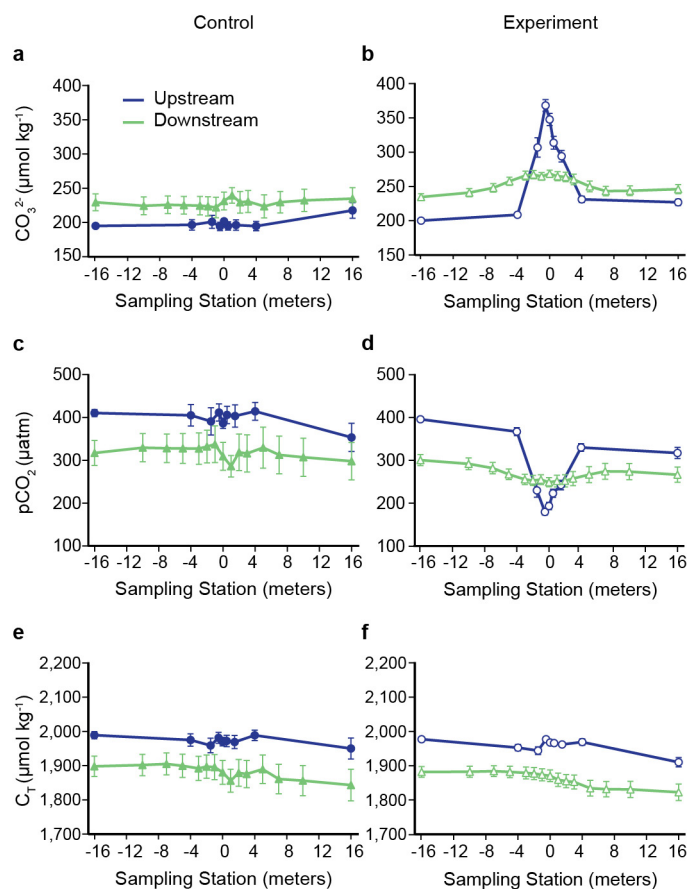
Extended Data Figure 1 | Theoretical representations of the null, H0, and alternative, H1, hypotheses. a, In H0, the reef does not take up added alkalinity; here, the change in alkalinity between the upstream and downstream transects would not be systematically related to the dye concentration, and the ratio of the alkalinity–dye relationship, r , would not be expected to change between the upstream and downstream locations (that is, $r_{up} = r_{down}$). **b**, In H1, reef uptake of added alkalinity occurs; here, areas with more alkalinity (and more dye) change at a different rate than areas with less alkalinity (and less dye), resulting in a change in the alkalinity–dye slope (that is, $r_{up} > r_{down}$).



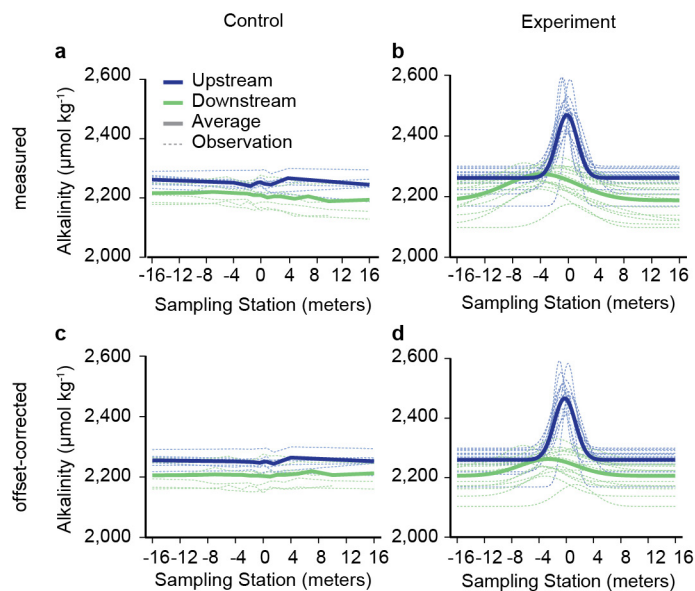
Extended Data Figure 2 | Community composition of the reef flat study area. Percentage cover by benthic type is as follows: crustose coralline algae (39%), live coral (17%), turf algae (16%), macroalgae (19%), sand/rubble (9%), and *Halimeda* (5%).



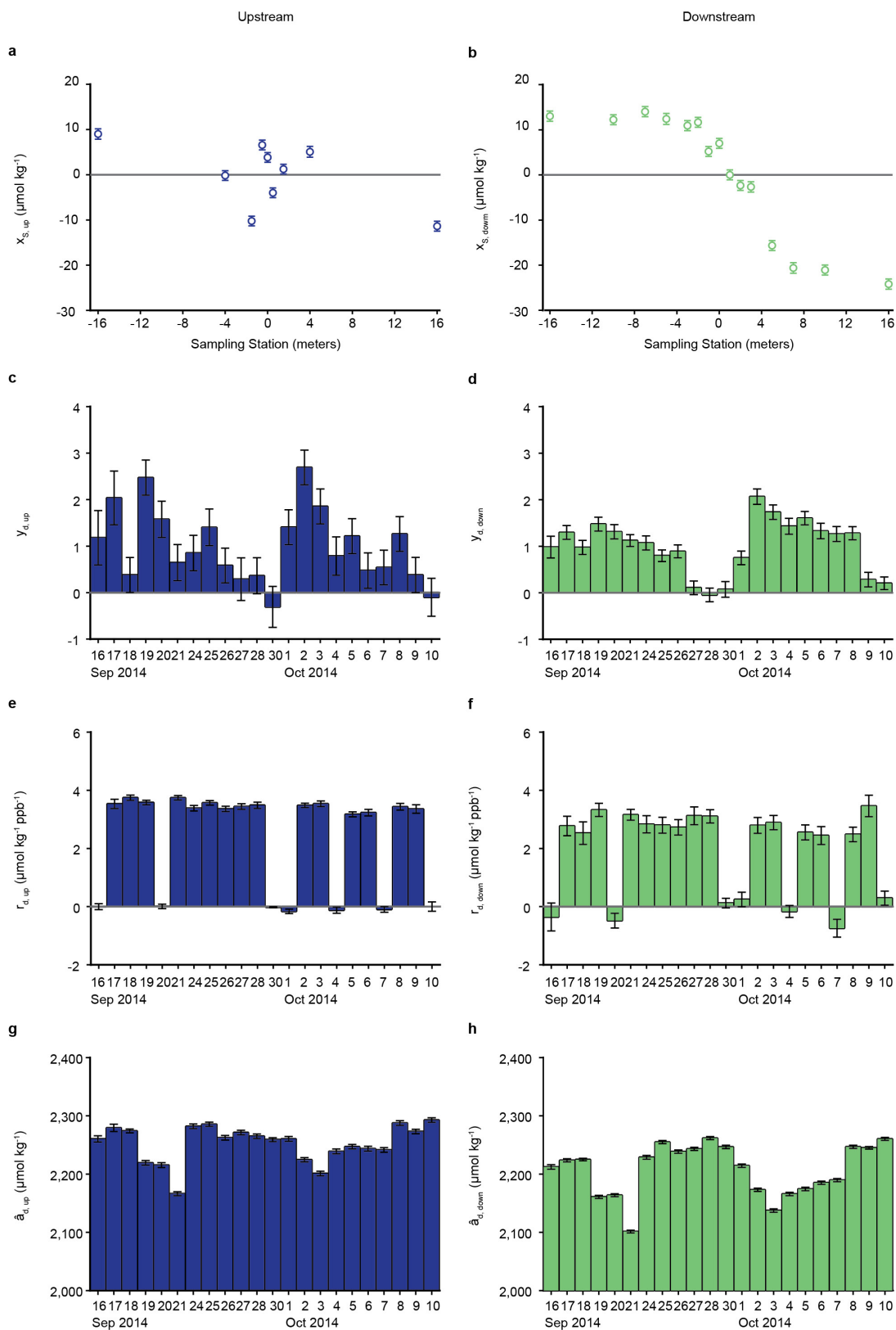
Extended Data Figure 3 | Schematic of study area showing meter-spacing of station locations for the 9 upstream (U) stations and 15 downstream (D) transects. Numbers indicate the metre-spacing from the centre of the study area, denoted as U0 for the upstream transect and D0 for the downstream transect. The outermost sampling locations for the upstream (-U16, U16) and downstream (-D16, D16) transects define the four outermost corners of the study area and were strategically positioned to lie outside the alkalinity-dye plume, rendering zero dye concentrations and added alkalinity.



Extended Data Figure 4 | Mean chemical conditions for control ($N = 7$) and experiment ($N = 15$) days. a, b, Carbonate ion concentrations ($[\text{CO}_3^{2-}]$); c, d, $p\text{CO}_2$; e, f, dissolved inorganic carbon concentrations (C_T) for upstream and downstream transects. Error bars, which represent standard errors, are indicative of day-to-day and hour-to-hour variability (not measurement error); estimates of measurement error are provided in the Methods. Total alkalinity (A_T), dye concentration, aragonite saturation state (Ω_{arag}), and total pH (pH_T) are provided in Figs 2 and 3.



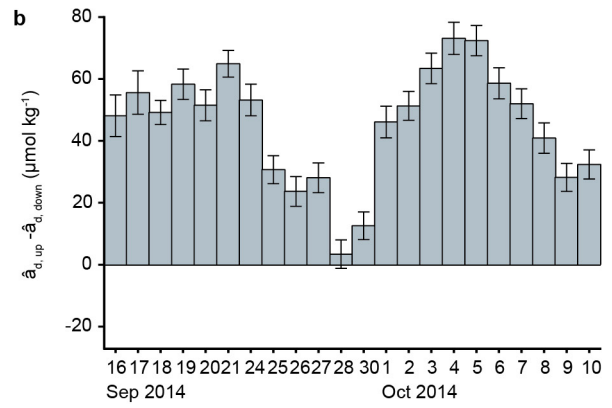
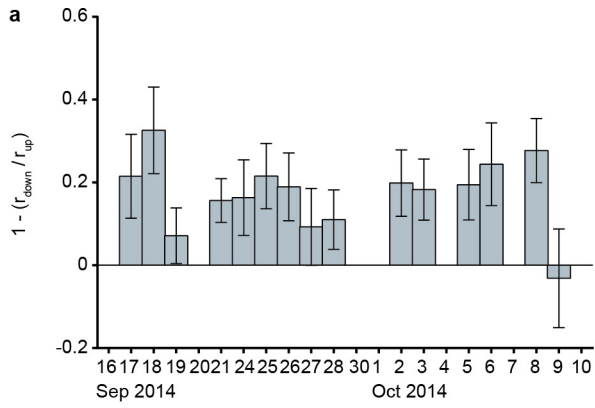
Extended Data Figure 5 | Comparison of alkalinity values before and after ‘offset-corrections’ used in the multivariate regression analysis. **a, b,** Measured (that is, ‘raw’) alkalinity values. **c, d,** ‘Offset-corrected’ alkalinity values. Bold lines represent average conditions; dashed lines show results by day. See Supplementary Information.



Extended Data Figure 6 | Results of the multivariate regression analysis.

a, b, Unique offsets by station, x_s , for the upstream and downstream transects. **c, d**, Magnitude of offsets by day, y_d , for upstream and downstream transects. **e, f**, Alkalinity-dye ratios by day, r_d , for upstream

and downstream transects. **g, h**, Mean background alkalinities by day, \hat{a}_d , for upstream and downstream transects. Error bars represent standard errors. See Supplementary Information.



Extended Data Figure 7 | Results of the multivariate regression were used to calculate the additional alkalinity uptake (that is, G_{increase}) and background alkalinity uptake (that is, $G_{\text{background}}$) by day. a, Fraction of added alkalinity taken up by the reef by day, given by $1 - (r_{\text{down}}/r_{\text{up}})$,

b, Background reef uptake by day, given by $(\hat{a}_{d,\text{up}} - \hat{a}_{d,\text{down}})$. Error bars represent standard errors. See Supplementary Information.

Extended Data Table 1 | Schedule for control and experiment days, including date, time, predicted height of low tide, and mean photosynthetically active radiation (PAR) for the 1 h study period

Date	Low Tide (HHMM)	Water Depth (m)	PAR ($\mu\text{mol m}^{-2} \text{s}^{-1}$)	Type of Study
16 Sept	0737	0.88	1146	Control
17 Sept	0907	0.93	1626	Experiment
18 Sept	1026	0.85	1797	Experiment
19 Sept	1125	0.72	1800	Experiment
20 Sept	1210	0.59	1715	Control
21 Sept	1249	0.47	1215	Experiment
24 Sept	1425	0.29	931	Experiment
25 Sept	1455	0.30	675	Experiment
26 Sept	1528	0.35	551	Experiment
27 Sept	1604	0.44	297	Experiment
28 Sept	1647	0.58	25	Experiment
30 Sept	0532	0.57	277	Control
01 Oct	0639	0.75	866	Control
02 Oct	0809	0.84	1459	Experiment
03 Oct	0940	0.80	1055	Experiment
04 Oct	1051	0.65	1916	Control
05 Oct	1150	0.46	1636	Experiment
06 Oct	1240	0.30	1707	Experiment
07 Oct	1327	0.19	1453	Control
08 Oct	1411	0.15	1179	Experiment
09 Oct	1455	0.19	787	Experiment
10 Oct	1539	0.29	513	Control

Tides were provided courtesy of One Tree Research Station. The low-tide time represents the time at which pumping onto the reef started; sampling occurred 60 min afterwards. Data for photosynthetically active radiation were obtained from the Australian Institute of Marine Science weather station at One Tree Island (<http://data.aims.gov.au/aimsrds/station.xhtml?station=131>). There was no significant difference between mean light levels for control ($1,166 \pm 217 \mu\text{mol m}^{-2} \text{s}^{-1}$, mean \pm s.e.m.) and experiment ($1,098 \pm 150 \mu\text{mol m}^{-2} \text{s}^{-1}$) days.

Extended Data Table 2 | Mean (± 1 s.e.m.) values for temperature (T), salinity (S), ammonium (NH_4), nitrite and nitrate ($\text{NO}_2 + \text{NO}_3$), and dissolved oxygen (DO) during the 22-day study period

	Control		Experiment	
	Upstream	Downstream	Upstream	Downstream
T ($^{\circ}\text{C}$)	23.0 ± 0.3	23.5 ± 0.5	23.3 ± 0.2	23.7 ± 0.3
S	35.79 ± 0.02	35.84 ± 0.02	35.71 ± 0.02	35.80 ± 0.02
NH_4 ($\mu\text{mol L}^{-1}$)	0.40 ± 0.02	0.23 ± 0.02	0.37 ± 0.01	0.24 ± 0.01
$\text{NO}_2 + \text{NO}_3$ ($\mu\text{mol L}^{-1}$)	1.14 ± 0.04	0.80 ± 0.02	1.08 ± 0.02	0.78 ± 0.01
DO (mg L^{-1})	5.9 ± 0.2	7.1 ± 0.4	6.2 ± 0.1	7.3 ± 0.1

Note that underlying natural variability (that is, day-to-day, hour-to-hour) contributes to standard errors; measurement errors for each parameter are indicated in the Methods.